



An assessment of physical development prediction in Shiraz (Iran) and its relationship with geomorphological factors

Khalil Valizadeh Kamran¹, Abuozar Nasiri², Rahman Zandi³, Najmeh Shafiei², Rababeh Farzin Kia²

¹University of Tabriz, Department of Remote Sensing and GIS, Iran, valizadeh.tabrizu.ac.ir

²Firouzabad Institute of Higher Education, Faculty of Geography, Iran, abuzarnasiri@gmail.com, najmeh@yahoo.com, r.farzinkiya@gmail.com

³Hakim Sabzevari University, Department of Remote Sensing and GIS, Iran, r.zandi@hsu.ac.ir

Cite this study: Kamran, K. V., Nasiri, A., Zandi, R., Shafiei, N., & Kia, R. F. (2022). An assessment of physical development prediction in Shiraz (Iran) and its relationship with geomorphological factors. *Advanced Remote Sensing*, 2 (2), 47-57

Keywords

Satellite images
Land use
Markov chain model
Shiraz
OLS model

Research Article

Received: 20.08.2022
Revised: 26.09.2022
Accepted: 01.10.2022
Published: 28.12.2022

Abstract

The development of cities and their environmental impacts have adverse consequences. However, it is possible to move toward sustainable development through knowledge and awareness of the urban areas, investigation, application, and optimal use of modern technologies and sciences. The current study examined the land-use changes of the city of Shiraz using remote sensing (RS) and geographical information system (GIS) to estimate the increase in the urban area, the reduction in agricultural and horticultural lands, the abuse of rangelands, and unauthorized construction in mountainous areas during 2000-2018. City development was determined in the time interval of 2025 using the maximum likelihood algorithm, supervised method, and Markov chain model. The relationship between land use and geomorphological factors was examined using the OLS method, the results of which showed an increase in the area of built-in land use and a decrease in the area of barren and agricultural lands in Shiraz during 2000-2018. Over the 7-year period, the area of built-in (36%), horticultural and agricultural (11%), barren (19%), and rangeland (46%) land use will change. According to the output of the OLS method, distance from the fault and distance from the channel had the highest impact on urban development risk compared to other parameters with the probability of 83% and 72% and error of 0.007 and 0.008, respectively.

1. Introduction

The contemporary urban world has, unfortunately, caused a distance from the natural environment and the unwanted acceptance of imbalances that stem from the asymmetric relationships between humans and urban space [1]. Urban land use is one of the most critical issues of modern life [2]. Urban development, which affects large areas of land, is important in low latitudes and particularly in developing countries whose urban growth has overtaken Europe and North America [3].

Physical development in Iranian cities has always been associated with changes in the urban structure due to geographical features, human density, population growth, and rural migration, leading to unbalanced urban development. Accordingly, the growth of urbanization over the past decades has been disproportionate to the ability to equip urban spaces and expand infrastructure, creating severe problems such as expensive housing, unemployment, and informal housing represented in the urban physical body [4]. It is necessary to consider hazards and seek risk-free conditions in urban planning and models of urban physical development to reduce the

vulnerability of the population and ensure future developments. Urban sprawl is a dominant phenomenon that has caused the occupation of more land in low-density compared to dense and compact cities [5]. Although man-made areas cover only 3% of the Earth's surface, they have had a significant environmental impact on a global and local scale [6]. For example, the proximity of urban areas to agricultural lands has resulted in very unfavorable environmental consequences such as desertification and soil erosion. Thus, access to up-to-date and accurate information on land-use change is necessary to understand and manage the outcomes of such changes [7-8]. The area of the city of Shiraz has increased significantly in recent years, and urban sprawl has caused various economic, environmental, and social consequences. The current study aims to investigate the urban development of Shiraz and the related risks in recent years.

Alansi et al. [9] investigated the land hazards of urban development in the Malaysian river basin using the GIS technique. Guan et al. [10] used the cellular automata model and Markov chain to model land-use changes and examine the balance of urban growth and environmental protection by 2069. The results of this study showed an increase in urban land use and a decrease in agricultural lands and forest coverage in the study area. Václavík and Rogan [11] used the Land Change Modeler to examine land use/land cover changes in the Olomouc Region of the Czech Republic. According to their results, 9% of the mixed forest had been transformed into a broadleaf forest, and the residential areas increased by 35%. Kuldeep and Kamlesh [12] prepared a land-use map for Uttarakhand using Landsat satellite images between 2000 and 2009. After classification and validation, the results showed a significant decrease in the forest and agricultural lands and a considerable increase in residential land use in less than a decade. Iqbal [13] examined the trend of land-use changes in the urban area of Chittagong in Bangladesh from 1989 to 2011 using Landsat TM. The results showed a 27% change in the area under study. De Oliveira Silveira et al. [14] used the object-based method and images of Landsat 8 and Sentinel to classify forest landscape vegetation in Brazil. Huo et al. [15] used Landsat satellite data and object-based classification method to study deforestation in the United States from 2003-2011. They reported an overall accuracy of 88.1% image classification and introduced the object-based method as a suitable method for monitoring forest land degradation.

2. Material and Method

2.1. Study area

Shiraz is one of the metropolises of Iran, the capital of Fars province, and located in southwestern Iran. This city is at an altitude of 1550 meters above sea level in the mountainous region of Zagros with a temperate climate. The city of Shiraz is the third largest city in Iran with an area of 348 km² and a population of 1547129. Shiraz is in longitude of 52°20' to 52°47' and latitude of 29°22' to 29°42'. The city is located on a plane with a mild slope (5%) from the west to the east, limited to Baba Kuhi, Kaftarak, and Bemo Mountains from the north, Sabzpooshan mountains from the south, Derak Mountain from the west, and Maharloo Lake from the east. The city is connected to Marvdasht from the north, Firoozabad from the south, Arsanjan and Sarvestan from the east, and Kazerun from the west (Figure 1).

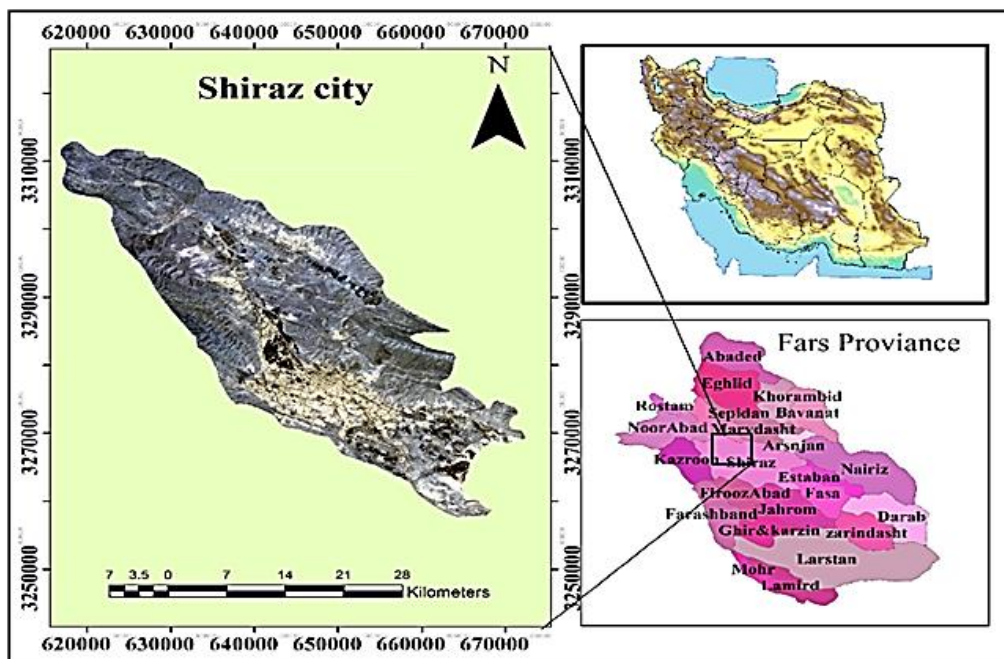


Figure 1. Location of the study area

This study used the images of the ETM sensor for 2000 and 2006 and the OLY sensor from Landsat 7 and 8 for 2018. The layer of distance from the fault and lithology from the 1:100000 geological map of Iran was used. The layer of distance from the channel, height, slope, and aspect provided from the DEM layer was used to examine the hazard and its role in urban physical development.

The dates of the images were 28.05.2000, 24.05.006, and 27.11.2019, respectively, and training samples were used to classify the pixels. Accordingly, the classification operation is performed in the form of intended training classes by defining specific pixels of the image for each class. The supervised algorithm (maximum likelihood) was used for classification. This method classifies the value of each unknown pixel based on its variance and covariance, after which its specific spectral response is analyzed. It is assumed that data of each class are distributed based on the normal distribution around the mean pixel of that class. In practice, the variance, covariance, and the mean of the different classes of each satellite image are calculated to classify the phenomena and assign each pixel to a class in which it is most likely to be present. Markov chain model was used to determine the changes in the land use in the study area (Shiraz), including horticultural and agricultural lands, urban areas, barren lands, and rangeland. The general flowchart of the research is shown in Figure 2.

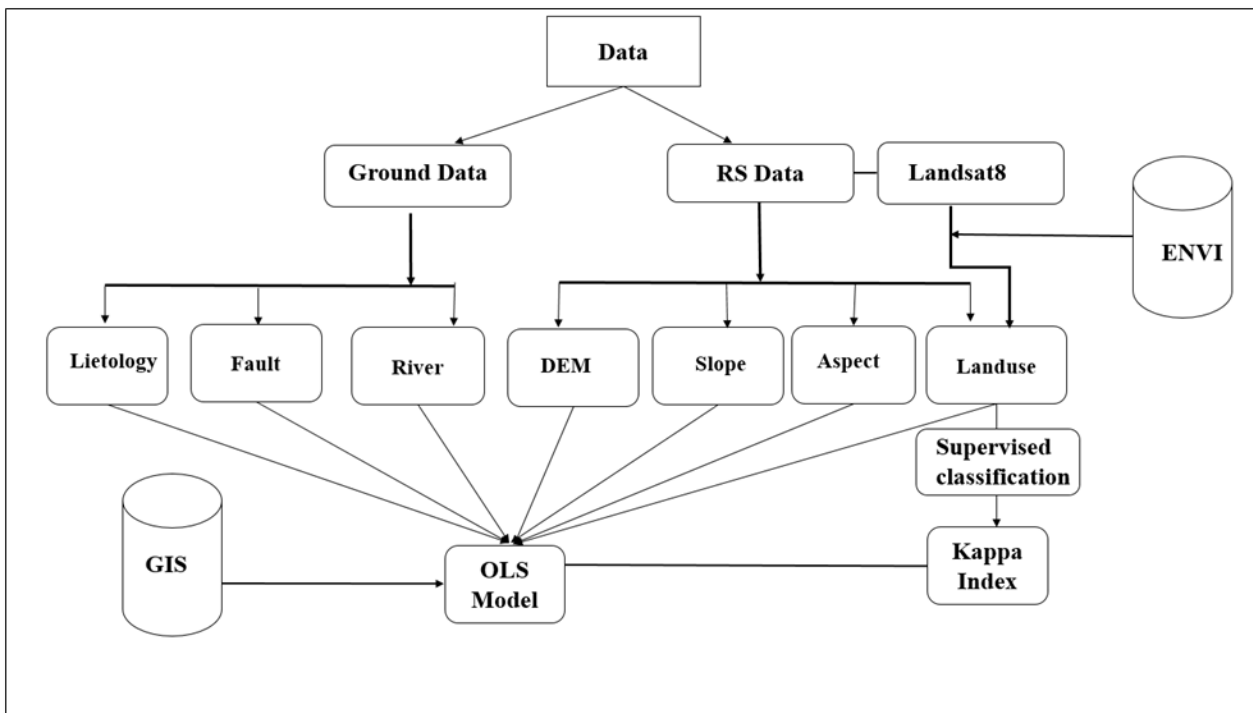


Figure 2. The general flowchart of the research

2.2. Markov Chain Model and CA-Markov

The Markov chain model operates as a random process in which the future state of a pixel depends only on its previous state, based on which it is predicted. The state transition probability matrix is the direct result of this model; however, there are no geographical interpretations in this model, and the model does not produce a single map indicating the spatial distribution of classes. John Von Neumann designed the CA-Markov model in the 1950s to add a spatial feature to the Markov model and address this problem [16]. Equation (1) is used to calculate prediction on the Markov model.

$$S(t+1) = P_{ij} \times s(t) \quad (1)$$

In which $s(t)$ and $s(t+1)$ indicate the system states at the time of t and $t+1$, respectively, and P_{ij} represents the transition probability matrix in a state, calculated by Equation (2).

$$P_{ij} = \begin{matrix} & p_{11} & p_{12} & \dots & p_{1n} \\ p_{2j} = & p_{21} & p_{22} & \dots & p_{2n} \\ & \dots & \dots & \dots & \dots \\ & p_{n1} & p_{n2} & \dots & p_{nn} \end{matrix} \quad (2)$$

In the Markov chain, land-cover classes are used as chain states. This analysis always uses 3-raster maps called models. In addition to these two maps, the CA Markov model also considers the time interval between the two images and the forecast time interval in the 2025 horizon. The output of the Markov model also includes the transition probabilities between states, the matrix of transitioned areas in each class, and finally the potentially conditional images for land use changes. Also, this study has used the Kappa index, which is calculated from the Equation 3, to ensure the classification.

$$\text{Kappa} = (P_0 - P_C) / (1 - P_C) * 100 \tag{3}$$

P0: Observed agreement
 PC: Expected agreement

2.3. The Results of Classification Accuracy

The calculation of the error matrix is one of the most widely used methods to assess classification accuracy. After the classification of the images, the kappa index and the overall accuracy of the classified maps were calculated based on the error matrix, indicating good agreement of the classification and the types of land-use classes. Table 1 shows the assessment of the classification accuracy of the satellite images. Accordingly, the overall accuracy is more than 90%, and the kappa index is between 0.88 and 0.9.

Table 1. The assessment of the classification accuracy of the satellite images

Years	Image	Kappa Index	Accuracy coefficient
2000	ETM	90/0	92%
2006	ETM	93%	94%
2018	OLI	88/0	91%

2.4 The Regression Model of Ordinary Least Squares (OLS)

The ordinary least square method (OLS) is the simplest and most common among the common regression models.

The idea behind the ordinary least square method is to assign values to the model coefficients that make the regression model closest to the observations, which means the least deviation from the observations. In spatial modeling with the OLS method, the coefficients or parameters of the statistical model are assumed constant concerning location (geographical coordinates). Therefore, the value of the dependent variable estimated by this model is for the whole study area. However, one of the drawbacks of this method in spatial modeling is the estimation of the same value for different parts of the area. The simple univariate linear regression model is as Equation 4:

$$\gamma_i = \beta_0 + \beta_1 x_i + \epsilon_i \tag{4}$$

In which, γ , x , ϵ , β_0 , and β_1 represent dependent variable (estimated), independent variable (estimator), error or model deviation in estimation, and model parameters or coefficients, respectively. the values of β_0 and β_1 are assumed to be constant for all the basin area. The statistical model of OLS and the matrix of model coefficient estimation are expressed by the following relations:

$$\beta^{\wedge} = (XTX)^{-1}XTy \tag{5}$$

$$y = X\beta + \epsilon \tag{6}$$

In which T, $(XTX)^{-1}$, and X indicate Matrix Transpose, inverse of variance-covariance matrix, and matrix of independent variables, respectively. The coefficients of the OLS multivariate regression model are constant across the location. It is not possible to map the spatial changes of the parameters or coefficients of the model using this model. Besides, this model is incompatible with ARC GIS software and does not consider spatial correlation [17].

3. Results

Given the changes in the city from 2000 to 2018, most of the urban development has occurred in the northwest direction. Barren land has undergone insignificant changes because most of the growth has been on horticultural, agricultural, and rangeland. According to the output of the maps in the three time periods of 2000, 2006, 2018, the

most land-use changes have been related to the built-in areas as a result of excessive construction, particularly from 2006 to 2018 in Shiraz, affecting other land uses adversely (Figures 3-5).

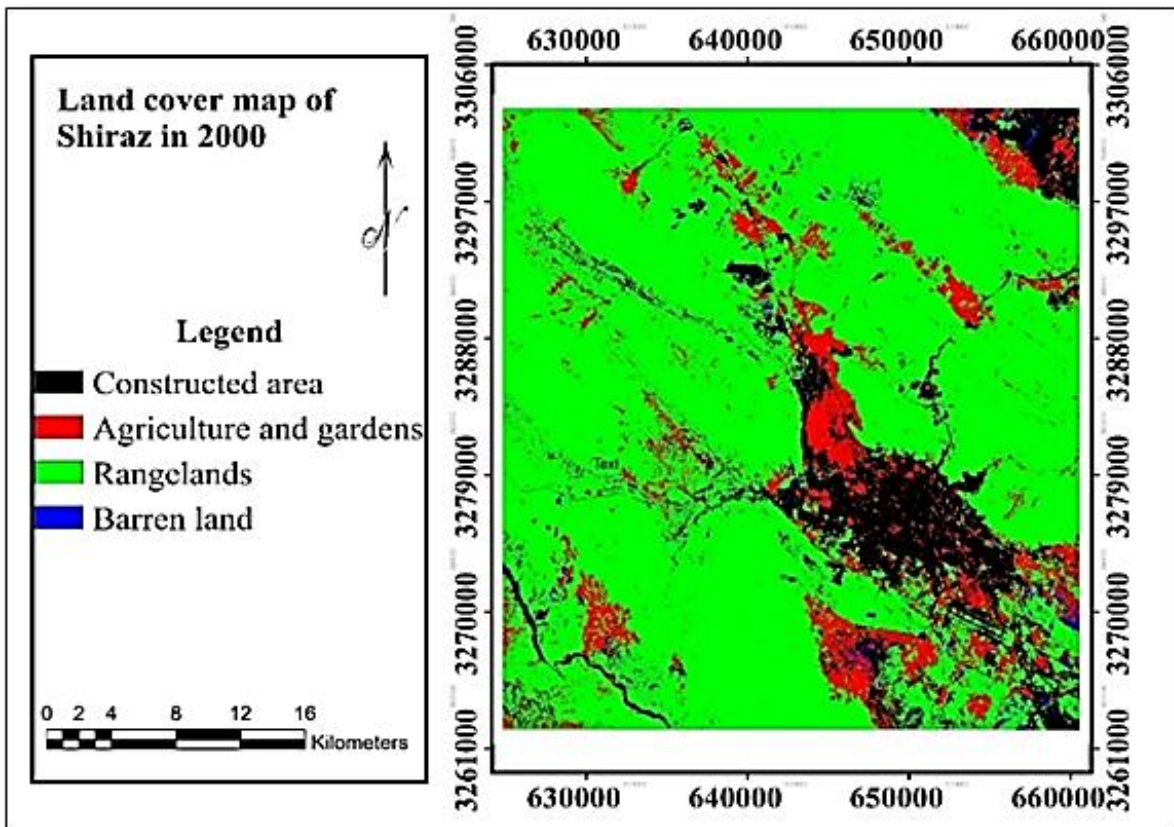


Figure 3. Land cover map of Shiraz city in 2000

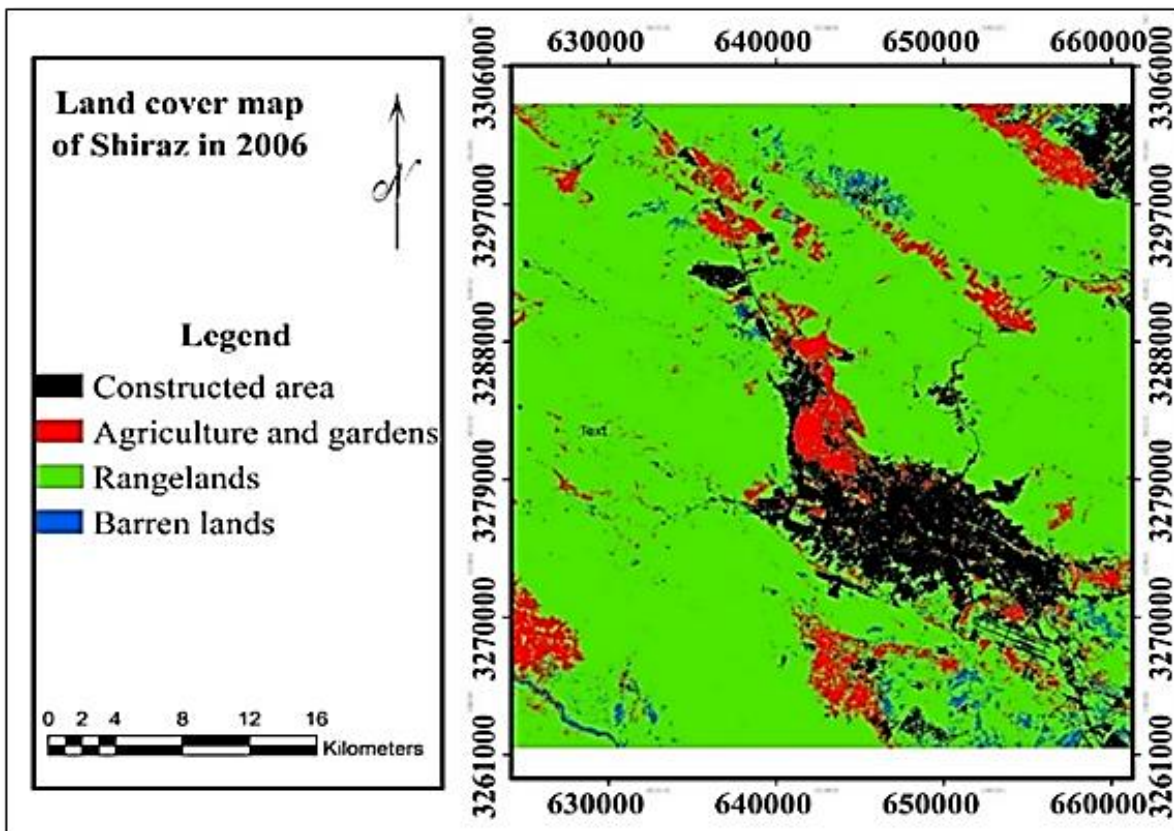


Figure 4. Land cover map of Shiraz city in 2006

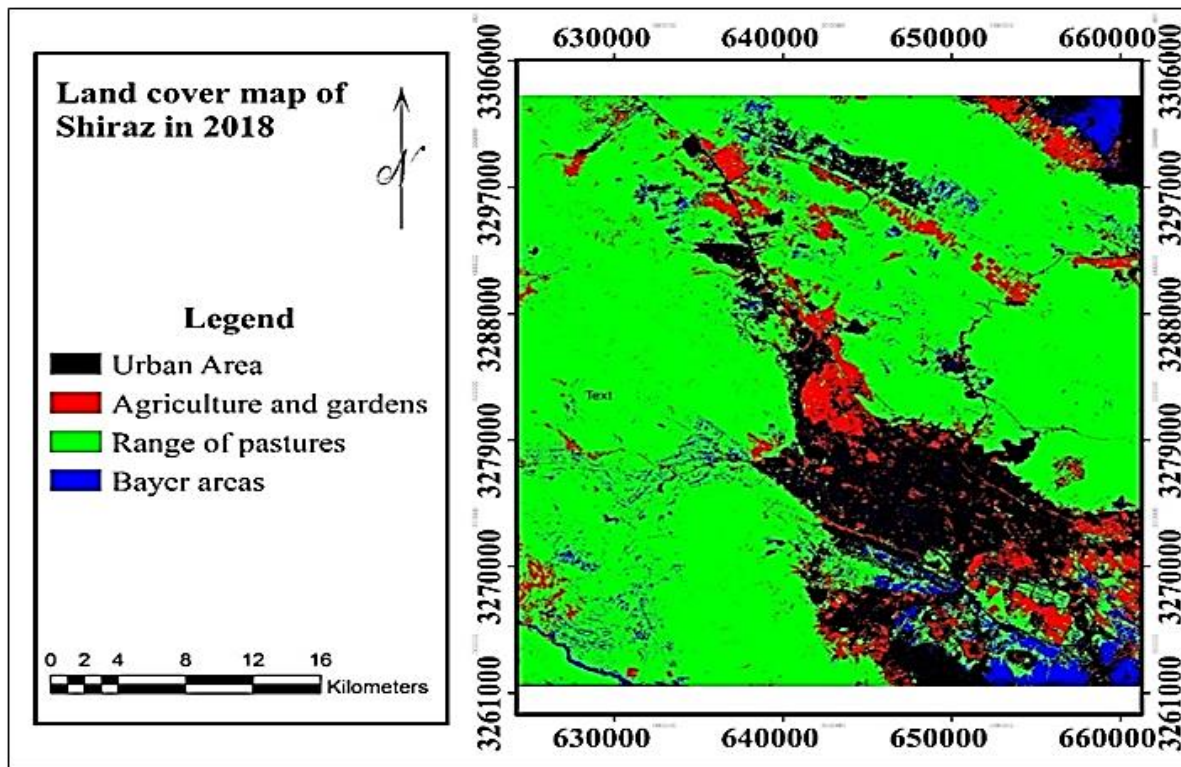


Figure 5. Land cover map of Shiraz city in 2018

3.1 State Transition Matrix

As shown in Table 2, the state transition matrix between 2000 and 2006 indicates that most changes have been from rangeland to horticultural and agricultural land use (84586 m²) and rangeland to built-in land use (83589 m²). Most agricultural land in Shiraz is allocated to horticulture; thus, rangeland has changed into built-in land use during this period.

Table 2. State Transition area matrix between 2000 and 2006 (in square meters)

Land cover	Built-in area	Gardens and Agriculture	Rangelands	Barren lands
Built-in area	160601	10935	16579	2422
Gardens and Agriculture	7547	108381	33851	1544
Rangelands	83589	84589	1499752	10064
Barren lands	11956	2410	24431	5229

According to Table 3, the highest probability of land use transition in the period 2006 to 2018 is related to the change of rangeland into horticultural and agricultural land use (and vice versa). From 2006 to 2018, the horticultural, agricultural, barren, and rangeland area has decreased, while urban area has increased to around 164477 m².

Table 3. State Transition area matrix between 2006 and 2018 (in square meters)

Land cover	Built-in area	Gardens and Agriculture	Rangelands	Barren lands
Built-in area	164477	22249	14926	15337
Gardens and Agriculture	7845	82282	66343	3047
Rangelands	6813	46075	139767	14262
Barren lands	11402	717	64707	11380

According to Table 4, the built-in area has followed an increasing trend in Shiraz from 2000 to 2018. The urban development of Shiraz is in the form of extensive and horizontal sprawl. Accordingly, the built-in area in Shiraz was 237, 271, and 316 km² in 2000, 2006, and 2018, respectively, indicating an approximately 79 km²-increase in the built-in area of Shiraz. On the other hand, the areas of horticultural and agricultural land, barren land, and rangeland have reduced from 2000 to 2018 due to the urban development of Shiraz. Table 4 indicates the area of each land use in 2000, 2006, and 2018. The table shows an increase in the area of built-in land and a decrease in

the area of rangeland from 2000 to 2018. The land uses of horticultural and agricultural on the one hand and barren land, on the other hand, have had reverse changes. From 2000 to 2006, the area of agricultural, horticultural, and barren lands has decreased while the area of rangeland has increased. However, in the next 10-year period, the urban area has increased, and the area of agricultural, barren, and rangeland has decreased. These changes are associated with the concentration of population and migration of people from the surrounding suburbs to the city of Shiraz, leading to the development of residential and commercial complexes by destroying horticultural and agricultural lands.

Table 4. Land area in 2000, 2006 and 2018 (in square meters)

Land cover	2000	2006	2018
Built-in area	237	271	316
Gardens and Agriculture	185	136	143
Rangelands	1471	1510	1318
Barren lands	173	39	79

3.2 Prediction of Land Use Classes by 2025

The Markov chain model was used to predict changes in the mentioned classes. The classification classes are used as chain states in this model. Also, the transition area matrix represents the area of the land use changed into another land use during 2000-2018. The area of the four land use classes was determined in the 2025 horizon using the output of the tables and the Markov chain model. These data determine the extent of built-in, horticultural and agricultural, barren, and rangeland classes in 2025 for the city of Shiraz (Figure 6). According to the area of land uses in 2018 and the prediction of their changes by 2025, the most changes have been in the built-in area with a 36% increase, after which the areas of barren land (19%), agricultural and horticultural land (11%), and rangeland (46%) have decreased. Among these, the changes in horticultural, agricultural, and barren lands are not significant (Table 5).

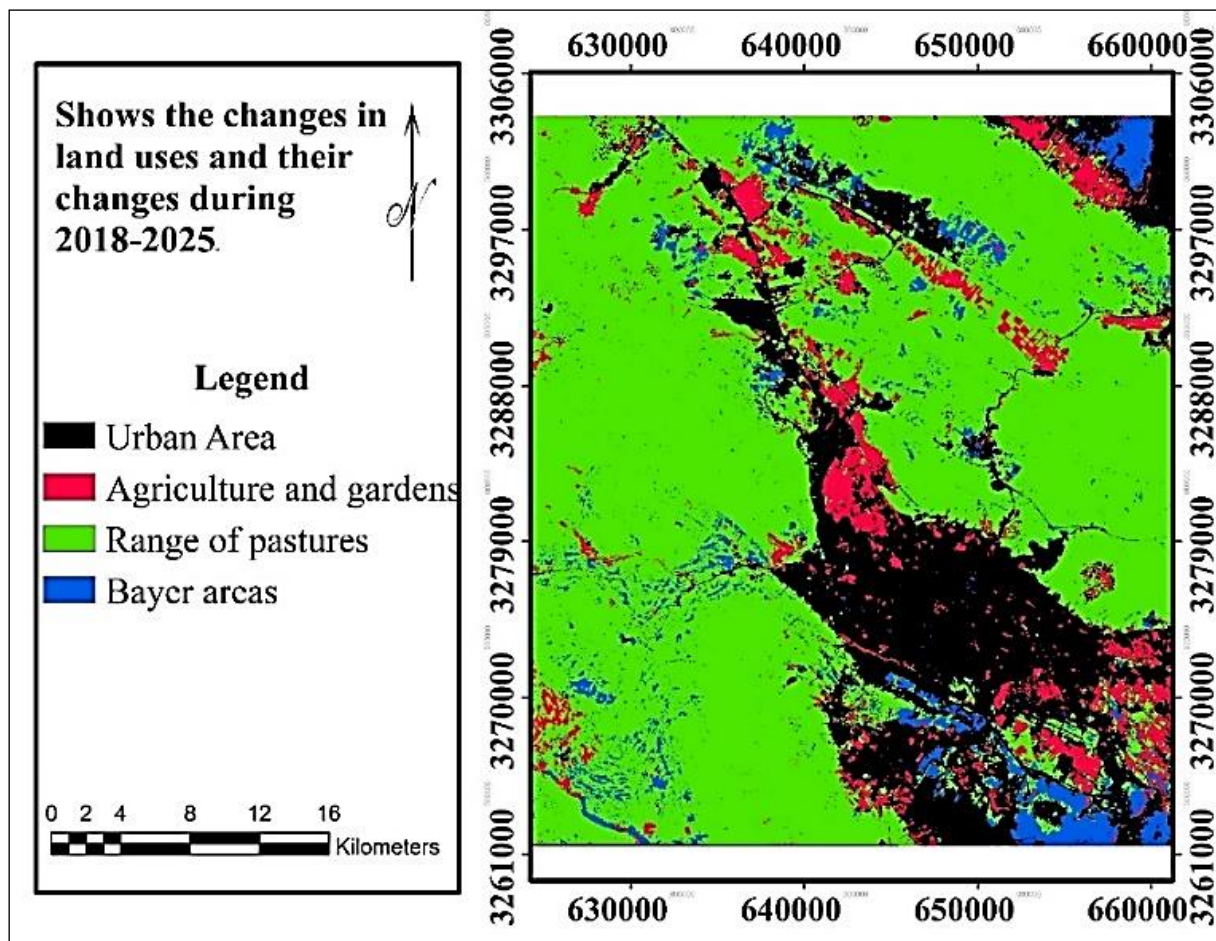


Figure 6. Different land uses and their changes in the study area during 2018-2025

Table 5. Prediction of Land Use Classes in the 2018- 2025 horizon

Land cover	2018	2025	Increase in changes in the 2025 horizon (in percent)
Built-in area	316197000	391657500	36%
Gardens and Agriculture	143565300	147025800	11%
Rangelands	1318344300	122972800	46%
Barren lands	79385400	89055900	19%

3.3 Elevation and Slope

Usually, the maximum suitable slope for urban planning is 9%, and values exceeding 9% increase urban development costs. Slopes close to zero bring about problems in terms of sewage disposal, leading to water pollution and area saturation when the groundwater level is high.

Therefore, urban development costs increase in these areas. The city of Shiraz has a normal slope in the range of 0-6 degrees, indicating that no serious hazards threaten the city. The city of Shiraz is located at an altitude of 1458 to 1892 meters, which is almost high. The central and southern parts of the city are much lower in height, and the northern areas have recently built towns at higher altitudes (Figure 7).

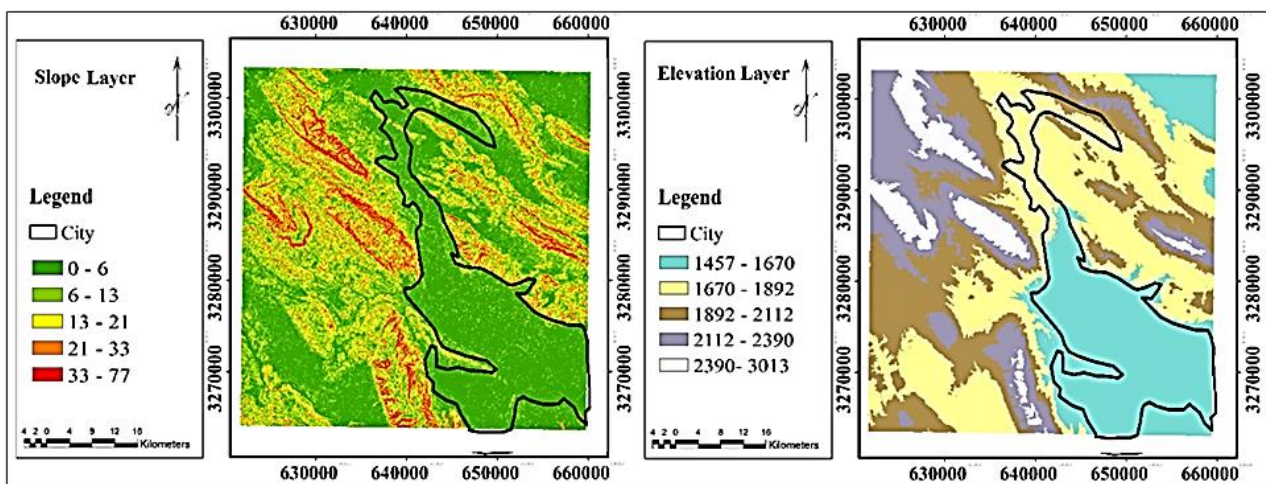


Figure 7. Layer of elevation and slop of Shiraz city

3.4 Lithology and Geomorphology

According to the lithology of the city, the southern, northern, and western parts are limited to calcareous formations, and the north and northwest of the city are limited to the Jahrom Lime Formation with resistant materials. According to satellite images in different years, the city has developed toward sediments inside calcareous formations in the mountainous areas, leading to adverse effects for the residents and different hazards such as earthquakes and landslides. Geomorphology is another influential parameter in the discussion of urban development. The geomorphology map of Shiraz indicated that the city has been formed in an alluvial fan and is suitable for urbanization (Figure 8).

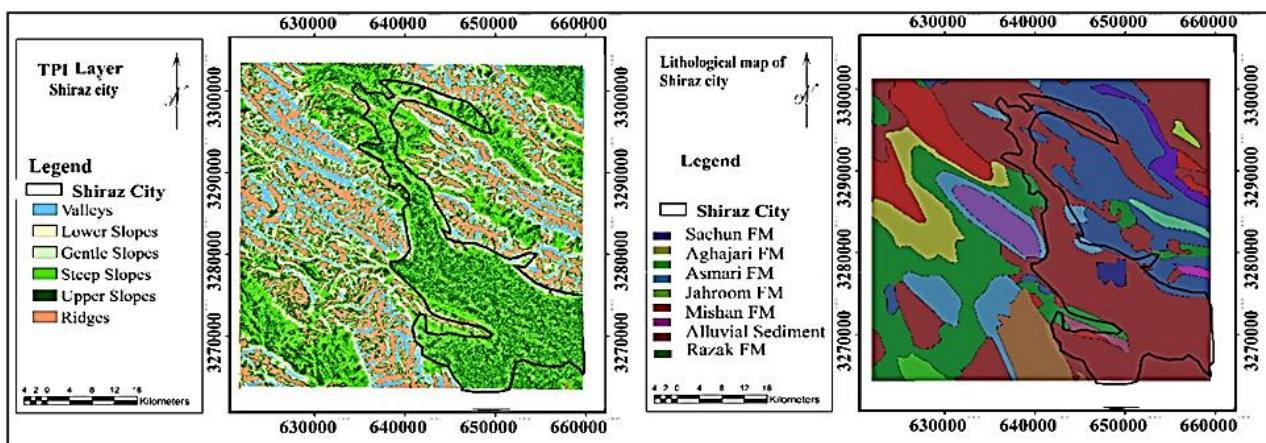


Figure 8. Lithology and geomorphology layer of Shiraz city

3.5 Fault and Channel

The fault is an influential factor in creating hazards, particularly in urban areas. Construction in the fault area and failure to avoid the proximity of fault can result in irreparable damage in the city of Shiraz. The current state of the city is the result of the changes in its urban physical body from 2000 to 2017. This fault, which was once far from the urban area of Shiraz, now passes through the new neighborhoods under construction in the north of the city because of the development of construction and towns on its territory. The development of the city toward the north is greatly important. The main river of Shiraz, which passes through the city center, has been dry in recent years due to successive droughts, but there are sometimes heavy rains in the area. However, the city has developed toward the river in recent years due to the failure to consider the appropriate distance from the channel. Construction in this direction leads to problems in the case of heavy rains and floods, along with the destruction of the buildings and irreparable damages due to the high speed of the flood. Another problem that can gradually lead to a crisis concerning these constructions is the inrush of sewage into residential and commercial units (Figure 9).

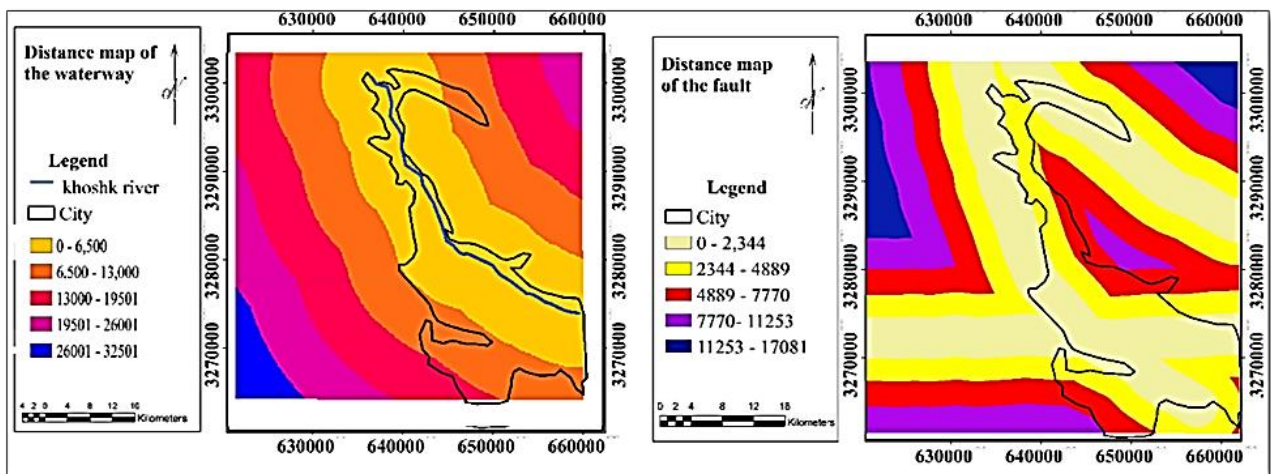


Figure 9. Distance map of the fault and distance map of the waterway of Shiraz city

3.6 Aspect

Aspect is an influencing factor in urban development. According to the aspect in the region, the southern slopes seem suitable for residential purposes and streets because of receiving more sunlight and appropriate airflow in the study area (Figure 10).

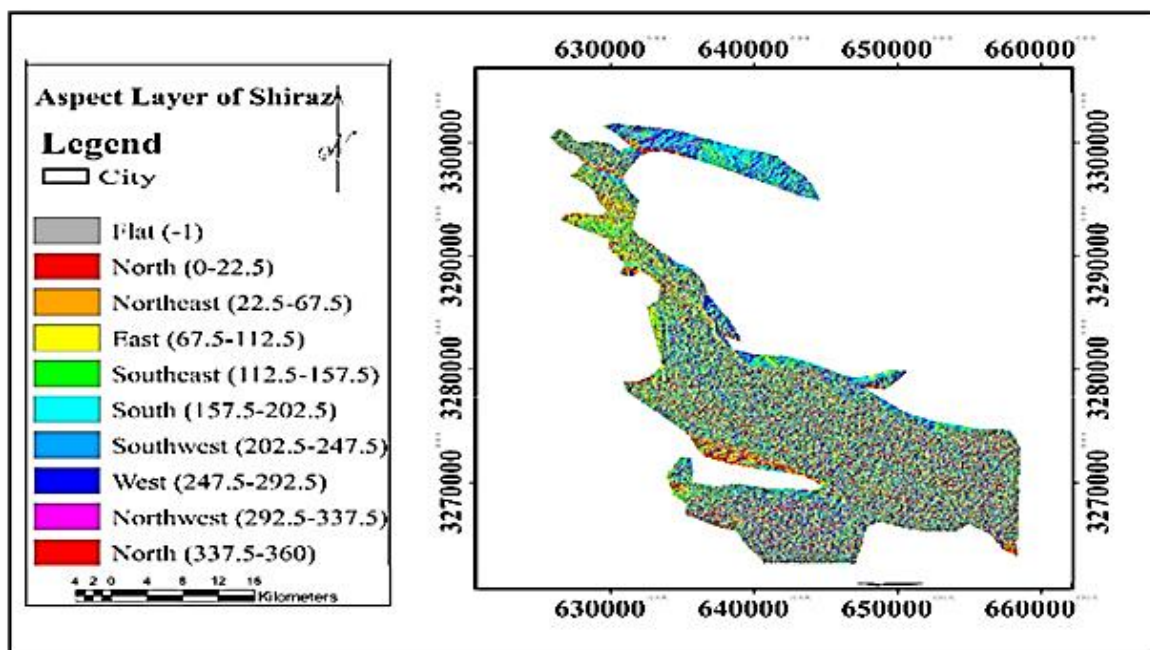


Figure 10. Aspect layer of Shiraz city

3.7 OLS Spatial Analysis

According to the results of the correlation between the land use layer and 7 parameters (height, slope, aspect, distance from the river, distance from the fault, lithology, and geomorphology), distance from the fault and distance from the channel had the greatest impact as environmental hazards on the development of Shiraz. Distance from the faults and distance from the channel had R² values of 83% and 72% with error percentages of 0.007 and 0.008, respectively, reflecting an effective role in the risk of urban development in Shiraz (Table 6).

Table 6. OLS model output

Variable	Coefficient [a]	Std Error	t-Statistic	Probability [b]	Robust SE	Robust_t	Robust Pr [b]	VIF [C]
Intercept	2.378635	0.819854	2.901293	0.006304*	0.889275	2.674803	0.011178*
Slope	-0.09494	0.107925	-0.87963	0.384893	0.072067	-	0.196057	1.248277
Dem	-0.07648	0.091327	-0.83746	0.407858	0.060733	1.317313	-	1.464532
Distance of River	0.075248	0.008121*	0.942644	0.352146	0.063551	1.259324	0.216018	1.278774
TPI	-0.11997	0.131355	-0.91332	0.367153	0.093836	1.184067	0.72067	1.168513
Distance of Fault	-0.03502	0.007982*	-0.43123	0.668874	0.085108	1.278485	-	1.099606
Aspect	-0.04579	0.049534	-0.92449	0.361388	0.034198	-0.41151	0.83138	1.136334
Lithology	0.138147	0.143937	0.959775	0.343571	0.22907	1.339092	0.188935	1.352305
						0.603078	0.550237	

4. Discussion and Conclusion

Urban life is expanding rapidly worldwide at a much faster pace in developing than developed countries. The process of urbanization in Iran is increasingly growing, leading to different problems and challenges. The horizontal development of cities leads to the destruction of lands around cities along with significant costs for the construction of towns and neighborhoods. It is possible to establish the dynamism and vitality of old neighborhoods by considering the neighborhood development capacities. It is also possible to prevent the destruction of suitable agricultural lands and the imposition of excessive costs through the application of sustainable urban development models. This study used satellite images from 2000 to 2018, supervised classification method (maximum likelihood algorithm), and Markov chain model to examine the changes in land coverage in horticultural, agricultural, built-in, barren, and rangeland uses. The study also investigated the relationship with geomorphological parameters such as height, slope, aspect, geomorphology, fault, channel, and lithology. In 2000, 2006, and 2018, the area of built-in land uses has changed in Shiraz with built-in, agricultural and horticultural, barren, and rangeland uses allocating 36%, 11%, 19%, and 46% to themselves, respectively. Considering the decentralized development of Shiraz, leading to urban sprawl and approaching the fault line and the main river, the risk of flood increases.

Over the 25-year period, agricultural land has become barren and vice versa. Residential land use had its maximum in 2018 (316000 km²) and is expected to reach 391000 km² by 2025. Shiraz has approached the main fault in the area because of horizontal expansion and unbalanced physical development, leading to erosion and destruction of buildings with weak infrastructure with a value of 88% and percentage error of 0.0007. These hazards cause irreparable damage; hence, the lands around the city of Shiraz (rainfed and irrigated agricultural land and rangeland) are considered critical areas in the future. In the case of incorrect planning, these areas will soon change their use, which is contrary to sustainable development. Thus, this important issue needs more attention from managers, planners, and those in charge of urban affairs. More control over urban areas, the use of mass and high-rise construction (compact city), the use of barren lands across the city (infill development), and directing urban development toward areas other than agricultural land should have priority to reduce the horizontal sprawl and the resulting problems and address the adverse environmental impacts, such as conversion and destruction of agricultural lands into urban lands, soil and water pollution, soil erosion, etc. According to the research findings, the following suggestions are the most important practical issues in urban and regional planning (urban engineering).

Funding

This research received no external funding.

Author contributions

Khalil Valizadeh Kamran: Data curation, Writing-Original draft preparation **Abouzar Nasiri:** Conceptualization, Methodology, Software. **Rahman Zandi:** Visualization, Investigation. **Najmeh Shafiei:** Visualization, Investigation, Writing-Reviewing and Editing. **Rababeh Farzin Kia:** Software, Validation.

Conflicts of interest

The authors declare no conflicts of interest.

References

1. Farid, Y. (1996). New Attitudes in the Context of Urban Geography. *Journal of Geographical Research*, Tehran, 33, 5-14.
2. Seif al-Dini, F. (2002). A dictionary of urban and regional planning. Shiraz, Iran: Shiraz University Press 1-507.
3. Chengtai D. (1999). Urban geomorphology in Chinese, 391.
4. Abedini, M., & Moghimi, E. (2012). the role of geomorphological bottlenecks in the physical development of metropolis of Tabriz for optimal use. *Geography and environmental planning*, 23(1), 147-166.
5. Bullard, R. D., Johnson, G.S., & Torres, A.O. (2000). *Sprawl City: Race, Politics, and Planning in Atlanta*, Island Press, Island, Washington, DC.
6. Herold, M., Goldstein, N. C., & Clarke, K. C. (2003). The spatiotemporal form of urban growth: measurement, analysis and modeling. *Remote sensing of Environment*, 86(3), 286-302.
7. Nasiri, A., Shirocova, V. A., & Zareie, S. (2019). Zoning of groundwater quality for plain Garmsar in Iran. *Water Resources*, 46(4), 624-629. <https://doi.org/10.1134/S009780781904002X>
8. Nasiri, A., Shafiei, N., & Farzin Kia, R. (2021). Investigation of Fahlian aquifer subsidence and its effect on groundwater loss. *Arabian Journal of Geosciences*, 14(7), 1-12. <https://doi.org/10.1007/s12517-021-06917-7>
9. Alansi, A. W., Amin, M. S. M., Halim, G. A., Shafri, H. Z. M., Thamer, A. M., Waleed, A. R. M., ... & Ezrin, M. H. (2009). The effect of development and land use change on rainfall-runoff and runoff-sediment relationships under humid tropical condition: Case study of Bernam watershed Malaysia. *European Journal of Scientific Research*, 31(1), 88-105. <http://psasir.upm.edu.my/id/eprint/17077>
10. Guan, D., Gao, W., Watari, K., & Fukahori, H. (2008). Land use change of Kitakyushu based on landscape ecology and Markov model. *Journal of Geographical Sciences*, 18(4), 455-468. <https://doi.org/10.1007/s11442-008-0455-0>
11. Václavík, T., & Rogan, J. (2009). Identifying trends in land use/land cover changes in the context of post-socialist transformation in central Europe: a case study of the greater Olomouc region, Czech Republic. *GIScience & Remote Sensing*, 46(1), 54-76. <https://doi.org/10.2747/1548-1603.46.1.54>
12. Tiwari, K., & Khanduri, K. (2011). Land use/land cover change detection in Doon valley (Dehradun tehsil), Uttarakhand: using GIS & Remote sensing technique. *International journal of Geomatics and Geosciences*, 2(1), 34-41.
13. Sarwar, M. I., Billa, M., & Paul, A. (2016). Urban land use change analysis using RS and GIS in Sulakbahar ward in Chittagong city, Bangladesh. *International Journal of Geomatics and Geosciences*, 7, 1-10.
14. de Oliveira Silveira, E. M., de Menezes, M. D., Júnior, F. W. A., Terra, M. C. N. S., & de Mello, J. M. (2017). Assessment of geostatistical features for object-based image classification of contrasted landscape vegetation cover. *Journal of Applied Remote Sensing*, 11(3), 036004. <https://doi.org/10.1117/1.JRS.11.036004>.
15. Huo, L. Z., Boschetti, L., & Sparks, A. M. (2019). Object-based classification of forest disturbance types in the conterminous United States. *Remote Sensing*, 11(5), 477. <https://doi.org/10.3390/rs11050477>.
16. Fan, F., Wang, Y., & Wang, Z. (2008). Temporal and spatial change detecting (1998–2003) and predicting of land use and land cover in Core corridor of Pearl River Delta (China) by using TM and ETM+ images. *Environmental monitoring and assessment*, 137(1), 127-147. <https://doi.org/10.1007/s10661-007-9734-y>
17. Erfanian, M., Hossein, K. M., Alijanpour, A. (2013). Introduction to OLS and GWR Multivariate Regression Methods in Spatial Modeling of Land Use Effects on Water Quality. *Journal of Watershed Management Promotion and Development*, 1(1).

